ON MULTIVARIATE FRACTIONAL BROWNIAN MOTION AND MULTIVARIATE FRACTIONAL GAUSSIAN NOISE

Jean-François Coeurjolly, Pierre-Olivier Amblard, Sophie Achard

GIPSAlab/CNRS UMR 5216/ BP46, 38402 Saint Martin d'Hères cedex, France
Jean-Francois.Coeurjolly@gipsa-lab.grenoble-inp.fr

ABSTRACT

Following recent works from Lavancier *et. al.*, we study the covariance structure of the multivariate fractional Gaussian noise. We evaluate several parameters of the model that allow to control the correlation structure at lag zero between all the components of the multivariate process. Then, we specify an algorithm that allows the exact simulation of multivariate fractional Gaussian noises and thus fractional Brownian motions. Illustrations involve the estimation of the Hurst exponents of each of the components.

1. INTRODUCTION

Functional Magnetic Resonance Imaging (fMRI) consists in observing the functional brain at low frequencies, around 2 Hertz. One time series for each anatomical region of the brain is recorded and the objective is to study the networks of propagation of information in the brain. In [2], the authors computed pairwise inter-regional correlations between wavelets coefficients in order to take into account the properties of long range dependence of the time series. Indeed, the fMRI time series are well modeled by a long range dependent Gaussian process [2]. In order to combine the multivariate and long range dependence properties of the fMRI time series, there is a need to develop models of multivariate Gaussian long range dependent processes.

Here, we concentrate on a model recently introduced in [6, 8] as a generalization of fractional Brownian motion (fBm) to multivariate fractional Brownian motion (vfBm). The definition is much wider in [6] whereas [8] concentrates on the covariance structure of multivariate processes that are jointly self-similar. Note that these works have closed links with the work of Stoev&Taqqu [10]. The process we study here is thus the particular Gaussian case. To develop model of multivariate Gaussian fractal noises needed to model fMRI signal, we particularly study the increments of the multivariate fractional Brownian motions. We exhibit interesting features of the covariance structure, such as long range dependence of marginals or long range interdependence between components. Furthermore, we specify the parameters in order to get a prescribed correlation structure between the components. We also develop an exact simulation algorithm based on the extension of Wood&Chan's method [12] to simulate univariate Gaussian signals to multivariate Gaussian random fields [3]. Some properties of the algorithm are discussed, especially conditions for exactness of the simulation. Finally we present several simulations to illustrate the sample paths of the processes, and to illustrate the good behavior of the simulation algorithm.

2. THE MULTIVARIATE FBM AND FGN

2.1 Model and properties

The fractional Brownian motion, as defined by Mandelbrot&Van Ness [9] is a causal linear transform of a Wiener process, with a kernel that respect self-similarity and which is parametrized by the self-similarity index H. This transform can be generalized in several ways, including time-varying index and non causal integration [10], or operator self-similarity [6]. Here, we concentrate on particular cases of the latter, and study the multivariate fractional Brownian motion defined *via* a causal integration of the mixing of independent Wiener processes. This comes after the work of Didier&Pipiras in [6] when we restrict the operators involved to be diagonal matrices. Let $x(t)$ of dimension p be defined as

$$x(t) = \int k_H(u,t) A_+ dW(u) \tag{1}$$

where W is a vector of p independent standardized Wiener processes or Brownian motions, A_+ is a $p \times p$ matrix of reals. H is a diagonal matrix of parameters $H_j \in (0,1), \forall j = 1,\dots,p$, and $k_H(u,t)$ is a matrix of kernels that reads $(t-u)_+^{H-1/2} - (-u)_+^{H-1/2}$. In this notation, $(a)_+ = \max(a,0)$ and t^H is understood as the exponential of a matrix $\exp(H\log(t))$. As seen in the stochastic integral representation (1) of the vfBm, $x(t)$ is a multivariate non-stationary Gaussian process with stationary increments. Moreover, the components of $x(t)$ are correlated, and the structure of the correlation is inherited from the presence of the mixing matrix A_+. And the correlation structure is sufficient to completely determine the process since it is Gaussian and zero mean (as a linear transform of a zero mean Gaussian process).

2.2 Covariances and cross-covariances

Let $r_{jk}(s,t) = E[x_j(s)x_k(t)]$ and $\gamma_{jk}(h) = E[\Delta x_j(t)\Delta x_k(t+h)]$ respectively denote the cross-covariance of the components j and k of x, and the cross-covariance of the increments of the components j and k. For the sake of simplicity, let $B_{jk} = B(H_j+.5, H_k+.5)$ where $B(x,y)$ is the beta function.

Let $\sigma_j, j = 1,\dots,p$ be positive numbers, and $\rho_{jk}, j = 1,\dots,p, k > j$ be real numbers in $[-1,1]$. Let the matrix A be defined for $j,k = 1\dots,p$ by

$$A_{jj} = \frac{\sigma_j^2 \sin(\pi H_j)}{B_{jj}} \tag{2}$$

 ISSN 2076-1465

$$A_{jk} = \begin{cases} \dfrac{\sigma_j\sigma_k\rho_{jk}\sin(\pi(H_j+H_k))}{(\cos(\pi H_j)+\cos(\pi H_k))B_{jk}} & \text{if } H_j+H_k \neq 1 \\ \dfrac{2\sigma_j\sigma_k\rho_{jk}}{(\sin(\pi H_j)+\sin(\pi H_k))B_{jk}} & \text{if } H_j+H_k = 1 \end{cases} \quad (3)$$

Then, *if A is positive-semidefinite*, the resulting process $x(t)$ defined by (1) with $A = A_+A_+^T$ is a vector of p correlated fBm of parameters $H_j, j = 1\ldots,p$, and the correlation matrix at zero lag of the increments, i.e. $\gamma(0)$, is given by $\gamma_{jj}(0) = \sigma_j^2$, $\gamma_{jk}(0) = \rho_{jk}\sigma_j\sigma_k$.

Moreover, we may derive the following computations. In the sequel, let $|h| \geq 1$. For $j = 1,\ldots,p$, the j-th component $x_j(t)$ of $x(t)$ is a fractional Brownian motion. Hence,

$$\begin{aligned} r_{jj}(s,t) &= \frac{\sigma_j^2}{2}\Big\{|s|^{2H_j}+|t|^{2H_j}-|t-s|^{2H_j}\Big\}, \\ \gamma_{jj}(h) &= \frac{\sigma_j^2}{2}\Big\{|h-1|^{2H_j}-2|h|^{2H_j}+|h+1|^{2H_j}\Big\}. \end{aligned}$$

Now, for $j \neq k$, two cases occur.

Case 1: $H_j+H_k \neq 1$,

$$\begin{aligned} r_{jk}(s,t) &= \frac{\sigma_j\sigma_k\rho_{jk}}{2}\Big\{c_{jk}(s)|s|^{H_j+H_k}+c_{kj}(t)|t|^{H_j+H_k} \\ &\quad -c_{kj}(t-s)|t-s|^{H_j+H_k}\Big\}, \\ \gamma_{jk}(h) &= \frac{\sigma_j\sigma_k\rho_{jk}}{2}\Big\{c_{kj}(h-1)|h-1|^{H_j+H_k}-2c_{kj}(h)|h|^{H_j+H_k} \\ &\quad +c_{kj}(h+1)|h+1|^{H_j+H_k}\Big\} \end{aligned}$$

with $c_{jk}(t) = c_{jk}\mathbf{1}_{R^+}(t) + c_{kj}\mathbf{1}_{R^-}(t)$ and $c_{jk} = 2\cos(\pi H_j)/(\cos(\pi H_j)+\cos(\pi H_k))$.

Case 2: $H_j+H_k = 1$

$$\begin{aligned} r_{jk}(s,t) &= \frac{\sigma_j\sigma_k\rho_{jk}}{2}\Big\{(|s|+|t|-|t-s|) \\ &\quad +f_{jk}\left(s\log|s|-t\log|t|-(t-s)\log|t-s|\right)\Big\} \\ \gamma_{jk}(h) &= \frac{\sigma_j\sigma_k\rho_{jk}f_{jk}}{2}\Big\{(h-1)\log|h-1|-2h\log|h| \\ &\quad +(h+1)\log|h+1|\Big\}, \end{aligned}$$

with $f_{jk} = 2/\pi\tan(\pi H_j)$. The case $H_j = H_k = 1/2$ is a particular case leading to $\gamma_{jk}(h) = 0$.

For details on the computations of $r_{jk}(s,t)$ we refer the reader to [8]. The calculation of $\gamma_{jk}(h)$ follows easily from the knowledge of $r_{jk}(s,t)$. The preceding results raise several remarks:

- A_{jj} can be obtained from A_{jk} when $j = k$ and $\rho_{jj} = 1$.
- The limit of A_{jk} when $H_j+H_k \to 1$ is equal to the definition of A_{jk} when $H_j+H_k = 1$. This can be easily verified using trigonometric identities to write the first as (forgetting σ's and ρ's) $\sin(\pi(H_j+H_k)/2)/\cos(\pi(H_j-H_k)/2)$ and the second as $1/\big(\sin(\pi(H_j+H_k)/2)\cos(\pi(H_j-H_k)/2)\big)$. Thus A_{jk} for $H_j+H_k = 1$ could have been defined by continuity.
- If $H_j = H_k$, we observe that $c_{jk}(t) = c_{jk} = 1$ which leads to $\gamma_{jk}(h) = \gamma_{kj}(h), \forall h$. Thus in this particular case, this cross-covariance function is proportional to the covariance of a fGn of parameter H_j.
- As $|h| \to +\infty$, we derive the following equivalences. Denote $f \sim g$ when $\lim f(h)/g(h) = 1$. For $j \neq k$ and $H_j+H_k \neq 1$, expanding $(1-1/h)^{H_j+H_k}$ allows to obtain

$$\gamma_{jk}(h) \sim \frac{\sigma_j\sigma_k\rho_{jk}c_{kj}(h)(H_j+H_k)(H_j+H_k-1)}{2}|h|^{H_j+H_k-2}$$

Setting $j = k$ and $\rho_{jj} = 1$ allows to recover the well-known asymptotic behavior for the covaraince of a monovariate fGn

$$\gamma_{jj}(h) \sim \frac{\sigma_j^2 2H_j(2H_j-1)}{2}|h|^{2H_j-2}$$

If $j \neq k$ and $H_j+H_k \neq 1$ but $H_j \neq 1/2$ we obtain

$$\gamma_{jk}(h) \sim \frac{\sigma_j\sigma_k\rho_{jk}f_{jk}\mathrm{sign}(h)}{2}|h|^{-1}$$

These equivalences allow to have interesting conclusions. Firstly, if $H_j = 1/2 = H_k$, the Brownian motions are uncorrelated, except at lag 0. When $H_j+H_k = 1$ but $H_j \neq 1/2$, the fractional Gaussian noises are long range interdependent since their cross-covariance is not summable. Note that in this case one fGn is long range dependent and the other is necessarily not.
When $H_j+H_k \neq 1$, the same conclusion may be drawn. If the two fGn are long range dependent ($H_j > 1/2$ and $H_k > 1/2$), then necessarily they are long range interdependent. Interestingly, two fGn can be long range inderdependent when only one is long range dependent.
- Behavior of $\gamma_{jk}(h)$: without loss of generality, let $h \geq 1$ and $\rho_{jk} \geq 0$. When $H_j+H_k \neq 1$

$$\gamma_{jk}(h) = \sigma_j\sigma_k\rho_{jk}c_{kj} \times \widetilde{\gamma}_{\frac{H_j+H_k}{2}}(h),$$

where $\widetilde{\gamma}_H(h)$ is the covariance function of a fGn with Hurst parameter H and with variance 1. Since, $\widetilde{\gamma}_H(\cdot)$ is a negative and increasing (resp. positive and decreasing) function when $H < 1/2$ resp. ($H > 1/2$), we may derive the following statement (by studying the sign of c_{kj}) illustrated by Fig. 1:

$$\gamma_{jk}(h) \begin{cases} \text{is negative and increasing} & \text{when } H_j < 1/2 \\ \text{is positive and decreasing} & \text{when } H_j > 1/2 \\ \text{equals zero} & \text{when } H_j = 1/2. \end{cases}$$

Let us underline that the study of the function $(h-1)\log(h-1)-2h\log(h)+(h+1)\log(h+1)$ leads to the same conclusion when $H_j+H_k = 1$.

2.3 Discussion on the non-negatitivity of A

The non-negativity condition of the matrix A defined by (2) and (3) is the main limitation of this model. In the general case, there is no general condition on the vector $H =$

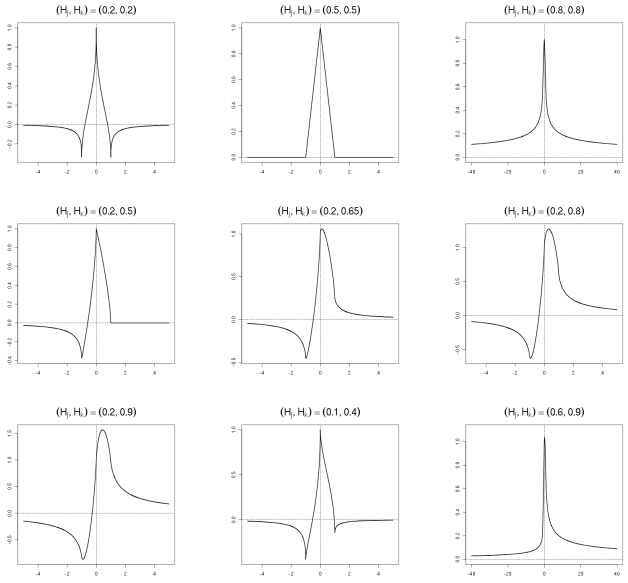

Figure 1: Examples of cross-covariance functions for different parameters H_j, H_k. Without loss of generality, the parameters σ_j, σ_k and ρ_{jk} are fixed to 1.

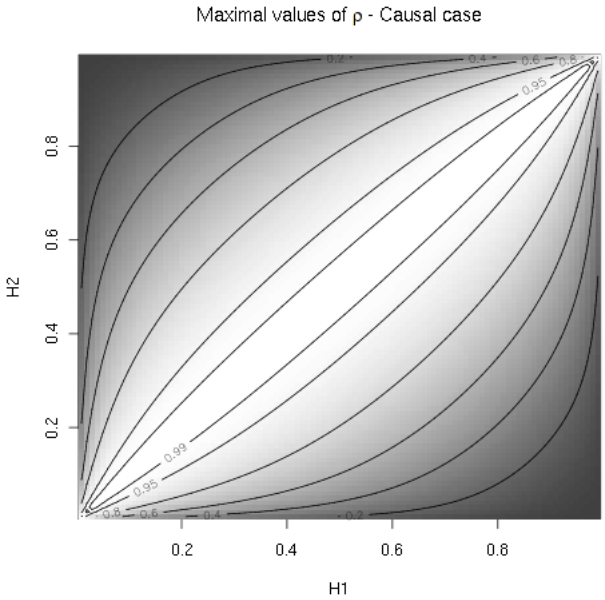

Figure 2: Maximal values of the absolute possible correlation parameter $|\rho_{12}|$ ensuring that the matrix A is positive, in terms of H_1 and H_2.

$(H_1,\dots,H_p)$ and on the matrix $\gamma(0)$ except if one assumes that $H_1 = \dots = H_p = \widetilde{H}$. Indeed, it is easily verified that $A = c(\widetilde{H}) \times \gamma(0)$ with $c(\widetilde{H}) = \sin(\pi\widetilde{H})/B(\widetilde{H}+.5, \widetilde{H}+.5)$ and so A is positive since $\gamma(0)$ is a covariance matrix. In this particular case, there is no limitation: $\widetilde{H} \in (0,1)$ and $\rho \in [-1,1]$.

In the simple case $p = 2$, the condition depends only on H_1, H_2 and $\rho = \rho_{12}$. A plot is feasible to determine the range of possible parameters, see Fig. 2. One observes that the more $|H_1 - H_2|$ is high (resp. low) the more the maximal possible correlation ρ is low (resp. high). For instance, for $H_1 = .1$, $H_2 = .9$, A is positive for $|\rho| \leq 0.11$ (approximately) and for $H_1 = .45$, $H_2 = .55$ this is true for $|\rho| \leq 0.97$ (approximately). Note that this sufficient condition when $p = 2$ is a necessary one when $p > 2$.

3. EXACT SIMULATION OF VFBM

3.1 Introduction

The exact simulation of fBm has been a question of great interest in the nineties. In principal this may be done by generating a sample path of a fractional Gaussian noise (fGn) which is more simple due to the stationarity of the increments. An important step towards efficient simulation was obtained after the work of Wood&Chan about the simulation of arbitrary stationary Gaussian sequences with prescribed covariance function [12]. The technique of Wood&Chan relies upon the embedding of the covariance matrix into a circulant matrix, a square root of which is easily calculated using the discrete Fourier transform. This leads to a very efficient algorithm, both in terms of computation time and storage needs. Wood&Chan methods provide an exact simulation method provided that the circulant matrix is definite positive, a property that is not always satisfied. However, for the fGn, it can be proved that the circulant matrix is definite positive for all $H \in (0,1)$ [5, 7].

In [3], Wood&Chan extended their method and provided a more general algorithm adapted to multivariate stationary random Gaussian signals. The main characteristic of this method is that if a certain non-negativity condition for a familiy of Hermitian matrices holds then the algorithm is exact in principal, i.e. the simulated data has the true covariance. We present hereafter the main ideas and briefly describe the algorithm.

3.2 Method and algorithm

In the sequel, the letter i is reserved for the complex number $\sqrt{-1}$. For a vector z and a matrix Q, $\bar{z}$ and $Q^\star$ respectively denote the conjugate of z and the conjugate transpose of Q. For two arbitrary matrices $A = (A_{jk})$ and B, we use $A \otimes B$ to denote the Kronecker product of A and B that is the block matrix $(A_{jk}B)$.

Let Δx denote the increments of a vfBm, that is a vectorial fractional Gaussian noise (vfGn) discretized at times $j = 0,\dots,n-1$. The covariance matrix G of Δx, given by $G = E[\Delta x \Delta x^T]$ is a $np \times np$ block matrix with each block $G(h)$ of dimension $p \times p$ given by $G(h) := G_{\ell,\ell+h} = E[\Delta x(\ell)\Delta x(\ell+h)^T] = \big(\gamma_{jk}(h)\big)_{j,k=1,\dots,p}$. The simulation problem can be viewed as the generation of a random vector following a $\mathcal{N}_{np}(0,G)$. This may be done by computing $G^{1/2}$ but the complexity of such a procedure is $\mathcal{O}(pn^3)$. To overcome this numerical cost, the idea is to embed G into the following block circulant matrix $C = circ\{C(j), j = 0,\dots,m-1\}$, where m is a power of 2 greater than $2(n-1)$ and where each $C(j)$ is the $p \times p$ matrix defined by

$$C(j) = \begin{cases} G(j) & \text{if } 0 \leq j < m/2 \\ \frac{1}{2}\big(G(j) + G(j)^T\big) & \text{if } j = m/2 \\ G(j-m) & \text{if } m/2 < j \leq m-1. \end{cases} \quad (4)$$

Such a definition ensures that C is a symmetric matrix with nested block circulant structure and that $G = \{C(j), j = 0,\ldots,n-1\}$ is a submatrix of C. Therefore, the simulation of a $\mathcal{N}_{np}(0,G)$ may be done by taking the n "first" components of a vector $\mathcal{N}_{mp}(0,C)$, which is done by computing $C^{1/2}$. The last problem is more simple since one may exploit the circulant characteristic of C: there exist m Hermitian matrices $B(j)$ of size $p \times p$ such that the following decomposition holds

$$C = (Q \otimes I_p)\, diag(B(j), j = 0,\ldots,m-1)\, (Q^\star \otimes I_p), \quad (5)$$

where Q is the $m \times m$ unitary matrix defined for $j,k = 0,m-1$ by $Q_{jk} = e^{-2i\pi jk/m}$. The computation of $C^{1/2}$ is much less expensive than the computation of $G^{1/2}$ since, as in the one-dimensional case ($p = 1$), (5) will allow us to make use of the Fast Fourier Transform (FFT) which considerable reduces the complexity.

Now, the algorithm proposed by Wood&Chan may be described through the following steps. Let m be a power of 2 greater than $2(n-1)$.

Step 1. For $1 \le u \le v \le p$ calculate for $k = 0,\ldots,m-1$

$$B_{uv}(k) = \sum_{j=0}^{m-1} C_{uv}(j) e^{-2i\pi jk/m}$$

where $C_{uv}(j)$ if the element (u,v) of the matrix $C(j)$ defined by (4) and put $B_{vu}(k) = B_{uv}(k)^\star$.

Step 2. For each $j = 0,\ldots,m-1$ determine a unitary matrix $R(j)$ and real numbers $\xi_u(j)$ $(u = 1,\ldots,p)$ such that $B(j) = R(j)\,\mathrm{diag}(\xi_1(j),\ldots,\xi_p(j))\,R(j)^\star$.

Step 3. Assume that the eigenvalues $\xi_1(j),\ldots,\xi_p(j)$ are non-negative (this will be discussed later) and define $\widetilde{B}(j) = R(j)\,\mathrm{diag}(\sqrt{\xi_1(j)},\ldots,\sqrt{\xi_p(j)})\,R(j)^\star$.

Step 4. For $j = 0,\ldots,m/2$ generate independent vectors $U(j),V(j) \sim \mathcal{N}_p(0,I)$ and define

$$Z(j) = \frac{1}{\sqrt{2m}} \times \begin{cases} \sqrt{2}U(j) & \text{for } j = 0, \frac{m}{2} \\ U(j) + iV(j) & \text{for } j = 1,\ldots,\frac{m}{2}-1, \end{cases}$$

let $Z(m-j) = \overline{Z}(j)$ for $j = \frac{m}{2}+1,\ldots,m-1$ and put $W(j) := \widetilde{B}(j)Z(j)$.

Step 5. For $u = 1,\ldots,p$ calculate for $k = 0,\ldots,m-1$

$$\Delta x_u(k) = \sum_{j=0}^{m-1} W_u(j) e^{-2i\pi jk/m}$$

and return $\{\Delta x_u(k), 1 \le u \le p, k = 0,\ldots,n-1\}$.

Step 6. For $u = 1,\ldots,p$ take the cumulative sums Δx_u to get the $u-th$ component x_u of a sample path of a vfBm.

3.3 Discussion

3.3.1 Computation cost

Let us concentrate on the computation cost of the most expensive steps, that is steps 1, 2 and 5. Step 1 requires $\frac{p(p+1)}{2}$ applications of the FFT of signals of length m, Step 2 needs m diagonalizations of $p \times p$ Hermitian matrices and Step 5 requires p applications of the FFT of signals of length m. Therefore, the total cost, $\kappa(m,p)$ equals

$$\kappa(m,p) = \mathcal{O}\left(\frac{p(p+1)}{2} m\log m\right) + \mathcal{O}(mp^3) + \mathcal{O}(pm\log m).$$

3.3.2 Semidefinite-positivity condition

The crucial point of the previous algorithm lies in the non-negativity of the eigenvalues $\xi_1(j),\ldots,\xi_p(j)$ for any $j = 0,\ldots,m-1$. In the one-dimensional case (when $p = 1$) Steps 2 and 3 disappear, and in Step 1, $B_{11}(k)$ corresponds to the $k-$th eigenvalue of the circulant matrix C_{11} with first line defined by $C_{11}(j) = \gamma_{11}(j)$ for $0 \le j \le m/2$ and $\gamma(m-j)$ for $j = m/2+1,\ldots,m-1$. For the fractional Gaussian noise, it has been proved by Craigmile for $H < 1/2$ [5], and by Dietrich&Newsam for $H > 1/2$ [7] that such a matrix is semidefinite-positive for any m (and so for the first power of 2 greater than $2(n-1)$. In the more general case $p > 1$, the problem is much more complex: the quantities $B_{uv}(k)$ are not necessarily real, and the establishment of a condition of positivity for the matrix $B_{uv}(k)$ does not seem obvious. When the condition in Step 3 does not hold, Wood&Chan suggest to either increase the value of m and restart Steps 1,2 or to truncate the negative eigenvalues to zero which leads to an approximate procedure. These problems will be deserved in a separate paper. Let us assert that for the simulation examples presented in the next section, we have observed that this condition is satisfied for m equal to the first power of 2.

4. SOME EXAMPLES

4.1 Bivariate fractional Brownian motion

Fig. 3 proposes some examples in the case $p = 2$. Except for the parameters $H = (0.2, 0.8)$ for $\rho = 0.9$ all the parameters satisfy the semidefinite-positivity condition on the matrix A defining the model and on the matrices $B(j)$ defined in Step 2 of the Wood&Chan's algorithm. We are then interested in retrieving the parameters based on a sample path. To estimate the Hurst exponents, we applied to each component of the vfBm an estimator built for the fBm, based on discrete variations [4]. To estimate the correlation parameter, we simply use the empirical correlation of the vfGn. Clearly, these estimators are naive and we hope to construct more adapted estimators by taking into account the behaviour of the cross-covariance for example. This interesting topic will be studied in a separate paper. The aim here is to have quickly an idea on the performance of the simulation method. The results are summarized in Fig. 4.

4.2 High dimensional fBm

We consider now a more complex vfBm with $p = 20$ components, $H_j = 0.7 + 0.1 \times (j-1)/19$, $\rho_{j,k} = 0.8$ and $\sigma_j = 1$ for $j,k = 1,\ldots,20$. A sample path is proposed in Fig 5. We have also performed a simulation based on $m = 200$ realizations. Denote by T_H and T_ρ the following statistics $T_H := \sum_{j=1}^{20}(\widehat{H}_j - H_j)$ and $T_\rho := \sum_{j=2}^{20}(\widehat{\rho}_{1j} - \rho_{1j})$. We obtain the results $\overline{T}_H = 5.02 \times 10^{-3}$ (resp. $\overline{T}_\rho = -0.023$) with a standard deviation of 0.046 (resp. 0.072).

Figure 3: Sample paths of length $n = 1000$ of a bivariate fractional Brownian motion with $\sigma_1 = \sigma_2 = 1$ for different Hurst parameters and for $\rho = 0.2$ (left) $\rho = 0.9$ (right).

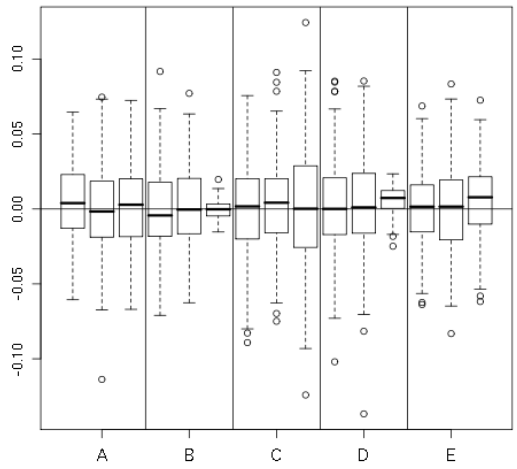

Figure 4: Boxplots of empirical biases of Hurst parameters and correlation coefficient based on $m = 200$ realizations of a vfBm of length $n = 1000$. The details of the parameters are the following: -A- $H = (0.2, 0.3)$, $\rho = 0.2$ -B- $H = (0.2, 0.3)$, $\rho = 0.9$ -C- $H = (0.7, 0.8)$, $\rho = 0.2$ -D- $H = (0.7, 0.8)$, $\rho = 0.9$ -E- $H = (0.2, 0.8)$, $\rho = 0.2$

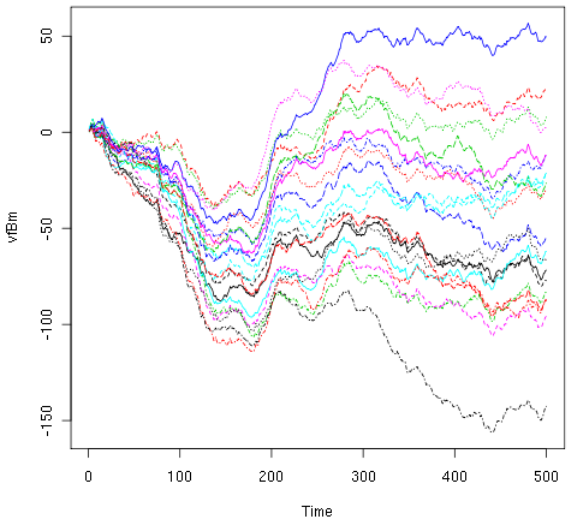

Figure 5: A sample path of a vfGn with $p = 20$ components of length $n = 500$ with $H_j = 0.7 + 0.1 \times (j-1)/19$, $\rho_{j,k} = 0.8$ and $\sigma_j = 1$ for $j,k = 1,\ldots,20$.

REFERENCES

[1] S. Achard, D. S. Bassett, A. Meyer-Lindenberg, and E. Bullmore. Fractal connectivity of long-memory networks. *Phys. Rev. E*, 77:036104, 2008.

[2] S. Achard, R. Salvador, B. Whitcher, J. Suckling, and E. Bullmore. A resilient, low-frequency, small-world human brain functional network with highly connected association cortical hubs. *The Journal of Neuroscience*, 26(1):63–72, 2006.

[3] G. Chan and A. Wood. Simulation of stationary gaussian vector fields. *Statistics and Computing*, 9(4):265–268, 1999.

[4] J. F. Coeurjolly. Estimating the parameters of a fractional brownian motion by discrete variations of its sample paths. *Statistical Inference for stochastic processes*, 4(2):199–227, 2001.

[5] P. Craigmile. Simulating a class of stationary gaussian processes using the davies-harte algortihm, with application to long memory processes. *Journal of Time Series Analysis*, 24:505–510, Jan 2003.

[6] G. Didier and V. Pipiras. Integral representations of operator fractional brownian motion. *Preprint*, 2009.

[7] C. R. Dietrich and G. N. Newsam. Fast and exact simulation of stationary gaussian processes through circulant embedding of the covariance matrix. *SIAM Journal on Scientific and Statistical Computing*, 18:1088???1107., 1997.

[8] F. Lavancier, A. Philippe, and D. Surgailis. Covariance function of vector self-similar processes. *Statistics and Probability Letters*, Jan 2009.

[9] B. Mandelbrot and J. Van Ness. Fractional Brownian motions, fractional noises and applications. *SIAM Rev.*, 10(4):422–437, 1968.

[10] S. Stoev and M. Taqqu. How rich is the class of multifractional brownian motions? *Stochastic Processes and their Applications*, 116:200–221, 2006.

[11] H. Wendt, A. Scherrer, P. Abry, and S. Achard. Testing fractal connectivity in multivariate long memory processes. *Proceedings of ICASSP*, page cdrom, 2009.

[12] A. Wood and G. Chan. Simulation of stationary gaussian processes in [0, 1] d. *Journal of computational and graphical statistics*, 3:409–432, 1994.